DALTON

Mono-, di-, and tri-nuclear complexes of iron(II) with *N*,*N*,*N*′,*N*′-tetramethylethylenediamine†

Sian C. Davies,[a] David L. Hughes,[a] G. Jeffery Leigh,*[,b] J. Roger Sanders[a] and Jaisa S. de Souza[c]

[a] *Nitrogen Fixation Laboratory, John Innes Centre, Norwich Research Park, Colney, Norwich NR4 7UH, UK*
[b] *School of Chemistry, Physics and Environmental Science, University of Sussex, Brighton BN1 9QJ, UK*
[c] *Departamento de Química, Universidade Federal do Paraná, Centro Politécnico, 81531-990 Curitiba-PR, Brasil*

Iron(II) chloride reacted with *N*,*N*,*N*′,*N*′-tetramethylethylenediamine (tmen) in tetrahydrofuran (thf) to give the mononuclear complex *trans*-[$FeCl_2(tmen)_2$] **1** and the dinuclear complex [{$FeCl(tmen)_2$}$_2$(μ-Cl)$_2$] **2**. Both adducts were characterised by microanalyses, magnetic measurements, Mössbauer spectroscopy, and crystal structure analysis. In solution in thf the two species are in an equilibrium affected by temperature and by concentration of tmen. Reaction of either **1** or **2** with Na[BPh_4] produced the trinuclear species [$Fe_3(\mu\text{-Cl})_3(\mu_3\text{-Cl})_2(tmen)_3$][$BPh_4$] **3**. This compound is paramagnetic both in the solid state and in solution. These iron complexes are very similar in structure to the corresponding vanadium complexes.

We have shown how the bulky diamine *N*,*N*,*N*′,*N*′-tetramethylethylenediamine (tmen) can assist the formation of trinuclear species of vanadium(II) from mononuclear species such as [$VCl_2(tmen)_2$].[1] The mechanism of such transformations has not been established, but we reasoned that it should involve an undetected dinuclear species, such as is well established in vanadium(II) chemistry, though not in the form of a tmen derivative.[2] If this is the case, then it might be possible to form a heterometallic trinuclear species by reaction of suitable mono- and di-nuclear species of different metals. The heterometallic species of greatest interest to us would contain both iron(II) and vanadium(II), because both these metals are involved in the recently established vanadium–iron nitrogenase.[3] However, iron(II) chloride complexes of tmen are not well known, and the only reference we could find is to an undefined material $FeCl_2(tmen)_n$, produced by direct reaction of iron(II) chloride with 5 molar equivalents of tmen.[4] It was used as a synthon for an iron(II) hydrocarbyl, [$Fe(CH_2Ph)_2(tmen)$], believed to have a distorted tetrahedral structure. We therefore commenced our studies by investigating the reaction of iron(II) chloride with tmen rather more closely. Our search for mixed iron(II)–vanadium(II) species is described elsewhere.[5]

Results and Discussion

Structures

Tetramethylethylenediamine reacts with anhydrous iron(II) chloride in 3:1 molar ratio in tetrahydrofuran (thf) to produce two complexes, as described in the Experimental section. The colourless compound **1**, proved to be [$FeCl_2(tmen)_2$], on the basis of crystal structural and micro-analysis. It is highly air- and moisture-sensitive, and is stable in solution only in an excess of tmen. Otherwise it forms the very pale green compound **2**, which was shown to be a dinuclear species [{$FeCl_2(tmen)$}$_2$(μ-Cl)$_2$], again on the basis of crystal structural and micro-analysis.

Complex **2** is usually the first product that crystallises from a warm reaction mixture containing an excess of diamine, while **1** is formed slowly at or below room temperature with incorporation of additional tmen. The formation of **1** occurs at the expense of **2**, and the equilibrium between them depends upon the temperature and the concentration of base. We have observed[1] a similar equilibrium involving mononuclear and trinuclear species in vanadium(II)–tmen chemistry.

Reaction of solutions of either **1** or **2** in thf with Na[BPh_4] in a 3:1 ratio of iron to tetraphenylborate produces crystals of [$Fe_3Cl_5(tmen)_3$][BPh_4] **3** in high yield. This behaviour is very similar to that observed in the vanadium system, and suggests that the M_3Cl_5 motif is common, at least among first transition series elements. We have since observed such a structure also in nickel chemistry,[6] and a cobalt analogue has just been reported.[7] We experienced some problems in characterising the very air-sensitive **3**. We were never able to observe a molecular ion in the FAB mass spectrum, in part because of sensitivity to the matrix, but we did observe an apparently characteristic peak at *m*/*z* at 553. This ion may well be produced in part by interaction with the matrix and we could not assign a structure to it. It was, however, useful for detecting **3** in mixtures.[5]

These three iron complexes have some intriguing structural features. They are, of course, not completely without precedent. Compound **1** would appear to be a typical high-spin octahedral iron(II) compound. Compound **2** has a dinuclear precedent in complexes such as [$Fe_2Cl_3(thf)_6$][$SnCl_5(thf)$], though the bridging is completely different.[8] We know of no iron precedent for compound **3**, but a tetranuclear species [$Fe_4Cl_8(thf)_6$] with bridging chlorides is well established.[9] Clearly there are classes of structure involving iron, chloride, and a neutral ligand of which examples of the first four members have been established. We now discuss our three new compounds in more detail.

Compound **1** crystallises in discrete octahedral molecules lying at centres of symmetry. Although there is some structural disorder in the tmen methylene bridges this was successfully modelled by assuming two possible orientations for the methylene carbon C(2), as shown in Fig. 1, and assigning occupancy factors of 50% to the atoms in each of these positions. This kind of phenomenon is not unusual in complexes with ligands such as tmen containing di(methylene) bridges.[1,10] The structural data are given in Table 1. The Fe–Cl bond length, 2.397(1) Å, is unremarkable, being in the range for octahedral high-spin Fe^{II} complexes.[11] It is significantly shorter, though, than the bonds in $FeCl_2$ (2.53 Å, octahedral microsymmetry),[12] and this indicates a substantial increase in the covalency of the bond.

† *Non-SI unit employed*: $\mu_B \approx 9.27 \times 10^{-24}$ J T^{-1}.

Table 1 Selected molecular dimensions (bond lengths in Å, angles in °) in *trans*-[$MCl_2(tmen)_2$] (M = Fe **1** or V[9]), with estimated standard deviations (e.s.d.s) in parentheses*

M = Fe		M = V	
Fe–N(1)	2.378(3)	V–N(1)	2.318(2)
Fe–N(2)	2.376(3)	V–N(2)	2.320(2)
Fe–Cl(3)	2.397(1)	V–Cl(1)	2.487(1)
N(1)–Fe–N(2)	79.2(1)	N(1)–V–N(2)	81.44(7)
N(1)–Fe–Cl(3)	89.9(1)	N(1)–V–Cl(1)	89.82(5)
N(2)–Fe–Cl(3)	90.0(1)	N(2)–V–Cl(1)	90.10(5)

* Torsion angles in the disordered tmen ligand in the Fe complex: N(1)–C(1)–C(2a)–N(2) 47.8(9), N(1)–C(1)–C(2b)–N(2) −44.5(11).

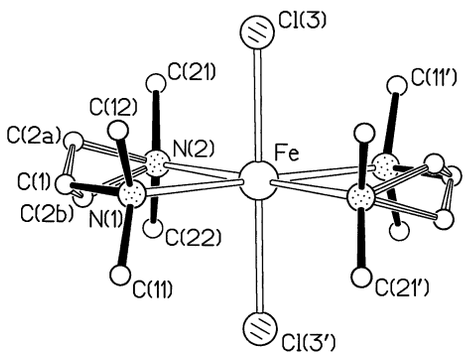

Fig. 1 Representation of the molecular structure of *trans*-[$FeCl_2(tmen)_2$] **1**, with the atom numbering scheme. The alternative sites which can be occupied by C(2a) and C(2b) in the disordered tmen bridges are depicted

Because the chloride ions occupy *trans* positions, the Fe–Cl bonds are not subjected to steric pressure, and, as expected, they are *ca.* 0.1 Å shorter than in the isostructural vanadium(II) complex, *trans*-[$VCl_2(tmen)_2$], the data for which are also included in Table 1.[10] The Fe–Cl(3) vector intercepts the equatorial plane at precisely 90°, as indicated by the angles N(1)–Fe–Cl(3) [89.9(1)] and N(2)–Fe–Cl(3) [90.0(1)°]. On the other hand, the N(1)–Fe–N(2) angle [79.2(1)°] deviates considerably from 90°, as in the vanadium case, and this is again probably a consequence of the small size of the chelate ring.

In **1** the Fe–N(1) and Fe–N(2) distances are identical within the experimental error [2.378(3) and 2.376(3) Å, respectively], and longer than the average V–N bond length in the vanadium homologue [2.319(2) Å].[10] This is presumably the result of strain due to co-ordination of the two tmen ligands. The high-spin Fe^{II} ion is smaller than V^{II} (ionic radii 0.78 and 0.88 Å, respectively).[13] Even so the metal–nitrogen bonds are longer than in [$VCl_2(tmen)_2$], probably in order to accommodate the amine molecules around the metal in the presence of the closer chlorides.

The analytical data obtained for complex **2** are consistent with the formulation [$Fe_3Cl_5(tmen)_3$]Cl, but the conductivity data are not. The crystal structure determination showed finally that '$FeCl_2(tmen)$' is actually the dinuclear [{$FeCl(tmen)\}_2(\mu$-$Cl)_2$]. There are two crystallographically independent (but chemically identical) molecules in the unit cell. One lies on a crystallographic centre of symmetry and is affected by disorder, whereas the other is pseudo-centrosymmetric and free of disorder. Fig. 2 is a representation of the pseudo-centrosymmetric dimer, and Table 2 presents selected molecular dimensions. The ratio of non-centrosymmetric to centrosymmetric molecules in the unit cell is 2:1. The disorder in the C(14)–N(13)–C(131)–C(132) portion of the tmen ligand in the centrosymmetric dimer was modelled assigning an occupancy factor of 0.5 to each of the possible orientations of C(14), C(131) and C(132). The tmen bridges assumed the usual conformation and dimensions, as found in the non-centrosymmetric molecule and in **1**.

Table 2 Selected molecular dimensions (bond lengths in Å, angles in °) in [{$FeCl(tmen)\}_2(\mu$-$Cl)_2$] **2** with e.s.d.s in parentheses*

Molecule 1, centrosymmetric			
Fe(1)···Fe(1′)	3.726(2)	Fe(1)–Cl(12)	2.266(2)
Fe(1)–Cl(11′)	2.345(2)	Fe(1)–N(13)	2.286(5)
Fe(1)–Cl(11)	2.648(2)	Fe(1)–N(16)	2.161(5)
Cl(11)–Fe(1)–Cl(12)	91.0(1)	N(13)–Fe(1)–N(16)	80.8(2)
Cl(11)–Fe(1)–N(13)	170.1(2)	Cl(11)–Fe(1)–Cl(11′)	83.7(1)
Cl(11)–Fe(1)–N(16)	90.7(1)	Cl(11′)–Fe(1)–Cl(12)	127.3(1)
Cl(12)–Fe(1)–N(13)	97.5(1)	Cl(11′)–Fe(1)–N(13)	95.0(2)
Cl(12)–Fe(1)–N(16)	120.2(1)	Cl(11′)–Fe(1)–N(16)	112.3(2)
Fe(1)–Cl(11)–Fe(1′)	96.4(1)		
Molecule 2, non-centrosymmetric			
Fe(2)···Fe(3)	3.732(1)		
Fe(2)–Cl(21)	2.650(2)	Fe(3)–Cl(31)	2.667(2)
Fe(2)–Cl(31)	2.341(2)	Fe(3)–Cl(21)	2.354(2)
Fe(2)–Cl(22)	2.264(2)	Fe(3)–Cl(32)	2.256(2)
Fe(2)–N(23)	2.280(5)	Fe(3)–N(33)	2.272(5)
Fe(2)–N(26)	2.172(5)	Fe(3)–N(36)	2.158(5)
Cl(21)–Fe(2)–Cl(31)	84.0(1)	Cl(31)–Fe(3)–Cl(21)	83.3(1)
Cl(22)–Fe(2)–Cl(21)	91.0(1)	Cl(31)–Fe(3)–Cl(32)	91.1(1)
Cl(22)–Fe(2)–Cl(31)	129.1(1)	Cl(32)–Fe(3)–Cl(21)	129.6(1)
Cl(22)–Fe(2)–N(23)	97.0(1)	Cl(32)–Fe(3)–N(33)	97.5(1)
Cl(22)–Fe(2)–N(26)	118.7(2)	Cl(32)–Fe(3)–N(36)	122.7(1)
N(23)–Fe(2)–N(26)	81.4(2)	N(33)–Fe(3)–N(36)	81.2(2)
N(23)–Fe(2)–Cl(21)	169.9(2)	N(33)–Fe(3)–Cl(21)	94.5(1)
N(23)–Fe(2)–Cl(31)	95.7(1)	N(33)–Fe(3)–Cl(31)	170.4(1)
N(26)–Fe(2)–Cl(21)	89.4(1)	N(36)–Fe(3)–Cl(21)	107.4(1)
N(26)–Fe(2)–Cl(31)	111.9(2)	N(36)–Fe(3)–Cl(31)	90.5(1)
Fe(2)–Cl(21)–Fe(3)	96.3(1)	Fe(2)–Cl(31)–Fe(3)	96.1(1)

* Torsion angles in the tmen ligands: N(13)–C(14a)–C(15)–N(16) 51.0(15), N(13)–C(14b)–C(15)–N(16) −42.4(16), N(23)–C(24)–C(25)–N(26) 52.2(11), N(33)–C(34)–C(35)–N(36) 48.5(12).

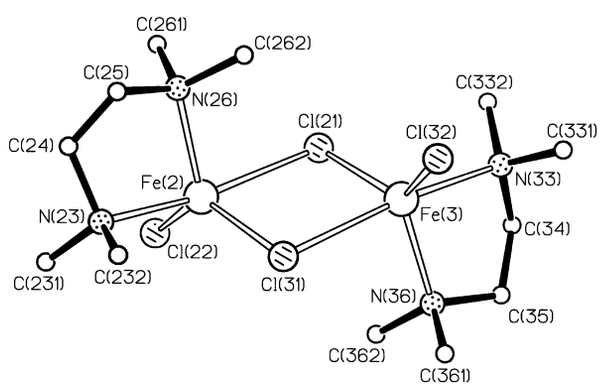

Fig. 2 Molecular structure of the non-centrosymmetric molecule of [{$FeCl(tmen)\}_2(\mu$-$Cl)_2$] **2**, showing the atom numbering scheme

Each Fe^{II} ion in **2** is five-co-ordinate and has distorted trigonal-bipyrimdal geometry, Fig. 2. For example, the co-ordination sphere around the Fe(3) is formed by a bridging chloride, Cl(31), and a nitrogen atom, N(33), in the axial positions, and by the remaining tmen nitrogen, N(36), a second μ-Cl, Cl(21), and the terminal chloride, Cl(32), in the equatorial plane. There is considerable distortion in both the axial and equatorial angles, due to the steric strain in the five-membered chelate rings.

The Fe···Fe distances in the crystallographically distinct molecules are 3.726(2) and 3.732(1) Å, very long for five-co-ordinate diiron(II) complexes containing bridging chloride ions.[14] We found a comparable separation only for [{$NiFe(L)Cl_2\}_2$] (3.725 Å) where H_2L = *N*,*N*′-bis(sulfanylethyl)-1,5-diazacyclooctane[15] in which the square-pyramidal high-spin iron(II) centres are antiferromagnetically coupled. The Fe···Fe

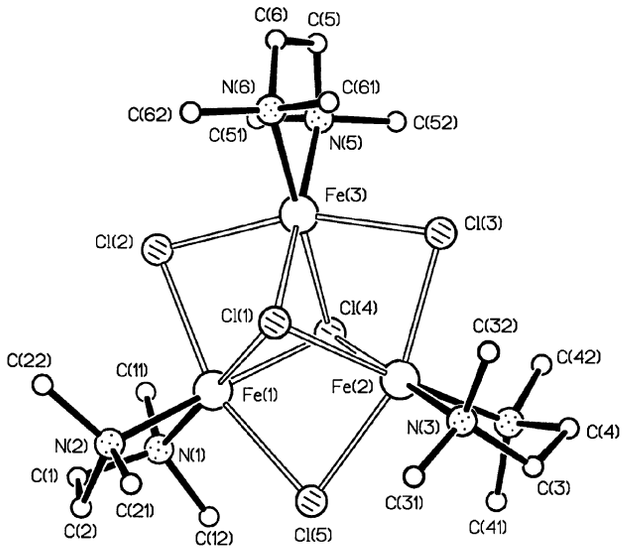

Fig. 3 View of the $[Fe_3(\mu\text{-}Cl)_3(\mu_3\text{-}Cl)_2(tmen)_3]^+$ cation in the tetraphenylborate salt **3**, with the atom numbering scheme

distance in **2** is much larger than the corresponding distance in $[Fe_2(\mu\text{-}Cl)_3(thf)_6]^+$ [3.086(2) Å], which is dinuclear both in solid state and in solution,[8] but the latter is cationic with three bridging chlorides. In the well known tetranuclear $[Fe_4Cl_8(thf)_6]$,[9] the mean distance between adjacent iron atoms (3.751 Å) is slightly longer than the Fe · · · Fe separation in **2**. These separations are, of course, far greater than any Fe · · · Fe bonding distance,[16] and it is therefore not surprising that the tetranuclear compound is said to exist only in the solid state, breaking into dinuclear species in thf solution.[9b]

In the cation $[Fe_2(\mu\text{-}Cl)_3(thf)_6]^+$, the six Fe–(μ-Cl) bond lengths are approximately equal,[8] and average at 2.488(9) Å. In contrast, the $\{Fe_2(\mu\text{-}Cl)_2\}$ core of **2** is highly asymmetric, with the $Fe\text{–}(\mu\text{-}Cl)_{ax}$ mean distance (2.655 Å) being much longer than the $Fe\text{-}(\mu\text{-}Cl)_{eq}$ (2.347 Å), and both longer than the average Fe–Cl(terminal) bond length (2.262 Å), as expected. The asymmetry arises because the bridging chloride atoms are axial to one metal atom and equatorial to the other.[14,17] Because of the unsymmetrical nature of the bridging and the large metal–metal separations, this kind of molecule has been stated to be comprised of 'loosely associated monomers' in the solid state.[17] We have magnetochemical evidence (see below) that dissociation does indeed occur in solution.

The diamine is not a particularly good electron donor or π-acceptor, and is unable to stabilise the four-co-ordinate '$FeCl_2$(tmen)' species. It is also probably less sterically demanding than dippe [1,2-bis(diisopropylphosphino)ethane]. The complex $[FeCl_2(dippe)]$[17] is one of the few examples of unequivocally characterised tetrahedral complexes, other than the tetrahalido complexes, of iron(II). A fine balance between electronic and steric properties is probably responsible for the structure of **2**, and of the related mononuclear and trinuclear species **1** and **3**.

In summary, tmen is not bulky enough to stabilise the electron-deficient tetrahedral $[FeCl_2(tmen)]$, too bulky to force a strong electronic interaction between metal ions in $[FeCl_2(tmen)_2]$, and just appropriate to form dimeric $[Fe_2Cl_4(tmen)_2]$ in the solid state. This molecule is probably also stable in solution in the absence of an excess of tmen or of another base/nucleophile at $T \leqslant 30$ °C. These features can be exploited in synthetic work.

The X-ray crystallographic analysis of **3** revealed four pairs of ions in the monoclinic unit cell, which is composed of $[Fe_3Cl_5(tmen)_3]^+$ cations and $[BPh_4]^-$ anions. The shortest intermolecular contact between the cation and the anion is 3.51(1) Å, from C(52) of a tmen ligand to the phenyl carbon atom C(744), Fig. 3 and supplementary data. Distances between anions are larger, the shortest being 3.666(8) Å between phenyl carbon atoms. Small intermolecular distances involving hydrogen atoms were also found. Although these values are smaller than the sum of the van der Waals radii for the atoms involved (3.7–4.0 for C · · · C and 2.4 Å for H · · · H contacts), they do not imply strong interactions, but rather considerable packing 'pressures' in the solid state.

Table 3 Selected molecular dimensions (bond lengths in Å, angles in °) in $[Fe_3Cl_5(tmen)_3][BPh_4]$ **3** with e.s.d.s in parentheses[a]

Fe(1) · · · Fe(2)	3.222(1)	Fe(1) · · · Fe(3)	3.248(1)
Fe(2) · · · Fe(3)	3.236(1)		
Fe(1)–Cl(1)	2.595(1)	Fe(2)–Cl(1)	2.591(2)
Fe(1)–Cl(2)	2.501(2)	Fe(2)–Cl(3)	2.501(2)
Fe(1)–Cl(4)	2.513(1)	Fe(2)–Cl(4)	2.552(2)
Fe(1)–Cl(5)	2.510(2)	Fe(2)–Cl(5)	2.481(2)
Fe(1)–N(1)	2.209(5)	Fe(2)–N(3)	2.202(5)
Fe(1)–N(2)	2.179(4)	Fe(2)–N(4)	2.180(5)
Fe(3)–Cl(1)	2.570(1)	Fe(3)–Cl(4)	2.574(1)
Fe(3)–Cl(2)	2.495(2)	Fe(3)–N(5)	2.196(5)
Fe(3)–Cl(3)	2.453(2)	Fe(3)–N(6)	2.197(5)
Cl(1)–Fe(1)–Cl(2)	81.4[b]	Cl(1)–Fe(2)–Cl(3)	81.5(1)
Cl(1)–Fe(1)–Cl(4)	87.0[b]	Cl(1)–Fe(2)–Cl(4)	86.3(1)
Cl(1)–Fe(1)–Cl(5)	81.7(1)	Cl(1)–Fe(2)–Cl(5)	82.3(1)
Cl(1)–Fe(1)–N(1)	179.4(1)	Cl(1)–Fe(2)–N(3)	94.7(1)
Cl(1)–Fe(1)–N(2)	95.4(1)	Cl(1)–Fe(2)–N(4)	177.4(1)
Cl(2)–Fe(1)–Cl(4)	82.7[b]	Cl(3)–Fe(2)–Cl(4)	82.5(1)
Cl(2)–Fe(1)–Cl(5)	158.6(1)	Cl(3)–Fe(2)–Cl(5)	159.1(1)
Cl(2)–Fe(1)–N(1)	98.8(1)	Cl(3)–Fe(2)–N(3)	97.8(1)
Cl(2)–Fe(1)–N(2)	98.4(1)	Cl(3)–Fe(2)–N(4)	96.1(1)
Cl(4)–Fe(1)–Cl(5)	83.5(1)	Cl(4)–Fe(2)–Cl(5)	83.3(1)
Cl(4)–Fe(1)–N(1)	93.6(1)	Cl(4)–Fe(2)–N(3)	179.0(1)
Cl(4)–Fe(1)–N(2)	177.4(1)	Cl(4)–Fe(2)–N(4)	94.3(1)
Cl(5)–Fe(1)–N(1)	98.3(1)	Cl(5)–Fe(2)–N(3)	96.6(1)
Cl(5)–Fe(1)–N(2)	96.0(1)	Cl(5)–Fe(2)–N(4)	100.3(1)
N(1)–Fe(1)–N(2)	84.0(2)	N(3)–Fe(2)–N(4)	84.7(2)
Cl(1)–Fe(3)–Cl(2)	82.0[b]	Cl(2)–Fe(3)–N(6)	97.6(2)
Cl(1)–Fe(3)–Cl(3)	82.8(1)	Cl(3)–Fe(3)–Cl(4)	83.0(1)
Cl(1)–Fe(3)–Cl(4)	86.3[b]	Cl(3)–Fe(3)–N(5)	97.3(2)
Cl(1)–Fe(3)–N(5)	178.3(1)	Cl(3)–Fe(3)–N(6)	98.1(2)
Cl(1)–Fe(3)–N(6)	95.2(1)	Cl(4)–Fe(3)–N(5)	95.4(1)
Cl(2)–Fe(3)–Cl(3)	159.0(1)	Cl(4)–Fe(3)–N(6)	178.2(1)
Cl(2)–Fe(3)–Cl(4)	81.6[b]	N(5)–Fe(3)–N(6)	83.1(2)
Cl(2)–Fe(3)–N(5)	98.3(1)		
Fe(1)–Cl(1)–Fe(2)	76.8[b]	Fe(1)–Cl(4)–Fe(2)	79.0[b]
Fe(1)–Cl(1)–Fe(3)	77.9[b]	Fe(1)–Cl(4)–Fe(3)	79.3[b]
Fe(2)–Cl(1)–Fe(3)	77.7[b]	Fe(2)–Cl(4)–Fe(3)	78.3[b]
Fe(1)–Cl(2)–Fe(3)	81.1(1)	Fe(1)–Cl(5)–Fe(2)	80.4[b]
Fe(2)–Cl(3)–Fe(3)	81.5(1)		

[a] Torsion angles in the tmen ligands: N(1)–C(1)–C(2)–N(2) 59.8(7), N(3)–C(3)–C(4)–N(4) −60.4(8), N(5)–C(5)–C(6)–N(6) 36.1(17). [b] E.s.d. is less than 0.05°.

The trinuclear cation shows the familiar *triangulo* arrangement seen in the vanadium(II) systems,[1] with the planar $\{Fe_3Cl_3\}$ core forming the equatorial plane of the molecule and the triply-bridging chlorides occupying the capping positions (Fig. 3). The co-ordination polyhedron around each Fe^{II} is a distorted octahedron, the donor atoms being two of the μ-Cl, both μ_3-Cl and the two N atoms of one tmen. A complete view of the cation with the numbering scheme is shown in Fig. 3. Table 3 contains selected interatomic distances and bond angles.

Complex **3** is isostructural with its vanadium homologue (Table 4). There are no large differences in the selected dimensions, that differ (at the most) by *ca.* 0.1 Å. The main distinction between the two complexes appears in the M · · · M non-bonding distances and in the $M\text{–}Cl_{cap}$ bonds, both being longer in the $\{Fe_3Cl_5\}^+$ core. As a consequence, and because the $M\text{–}Cl_{eq}$ bond lengths are very similar in the two complexes, the

Table 4 Comparison of mean principal bond lengths (Å) and angles (°) in the *triangulo*-$[M_3Cl_5(tmen)_3][BPh_4]$ complexes (M = V[1] or Fe)

Complex	M = V[1]	M = Fe
M · · · M	3.142(7)	3.235(8)
$M–Cl_{eq}$	2.500(4)	2.490(8)
$M–Cl_{cap}$	2.519(6)	2.566(12)
M–N	2.214(2)	2.194(5)
$Cl_{cap} \cdots Cl_{cap}$	3.497(1)	3.518(2)
$Cl_{eq}–M–Cl_{eq}$	162.1(2)	158.9(2)
$Cl_{cap}–M–Cl_{cap}$	87.9(6)	86.5(2)
N–M–N	82.8(3)	83.9(5)
$Cl_{eq}–M–Cl_{cap}$	83.6(2)	82.4(2)
$M–Cl_{eq}–M$	77.8(1)	81.0(3)
$M–Cl_{cap}–M$	77.1(2)	78.2(4)

octahedral geometry about each Fe^{II} ion is even more distorted than in the tris-vanadium cation, with smaller $Cl_{eq}–M–Cl_{eq}$ angles [158.9(2) *vs.* 162.1(2)°]. The bond lengths and angles involving the N-donor atoms in the tmen ligand are not significantly affected, unlike in $[MCl_2(tmen)_2]$, where the Fe–N bond is longer than the V–N bond. In terms of reactivity, the tris-iron(II) complex is probably subjected to higher ring strain caused by the longer Fe · · · Fe non-bonding distances, which could result in more facile substitution of the capping ligands or rupture of the trinuclear core in the presence of donors better than Cl^- or tmen.

Magnetic and spectral properties

Compound **1** is a normal paramagnetic solid with a temperature-independent magnetic moment in the solid state of 5.3 μ_B. A slight, reversible temperature dependence was observed in solution measurements, which can be explained by a small degree of association, perhaps involving loss of tmen from the co-ordination sphere. The ^1H NMR spectrum gave no indication of unexpected broadening, which could have been caused by the presence of ferromagnetic species due to oxidation or decomposition.

The magnetic behaviour of **2** is considerably more complicated. The solid-state data are shown in Fig. 4(*a*). The slight increase in μ_{eff} as the temperature is lowered from room temperature to 96 K is not really significant and it was found to be independent of field. Thus this behaviour in unexceptional. However, the situation in solution is quite different.

When the magnetic susceptibility was first determined in $[^2H_8]$thf solution in the range −100 to 40 °C (173–313 K), the measurements above room temperature produced data points clearly displaced from the straight line drawn through the remaining data. This was reproducible with different samples prepared by an alternative method. A more detailed investigation was then carried out in the range −50 to +50 °C (223–323 K), with determination at 3° intervals from 25 to 50 °C [Fig. 4(*b*)]. The plot indicates ferromagnetism because the experimental values of μ_{eff} (per Fe^{II} ion) increase with decreasing temperature. Fig. 4(*b*) also shows a small, reproducible, discontinuous transition above room temperature. Preliminary data suggest some thermal hysteresis associated with this change,[18] which we are investigating further.

These results are not particularly easy to explain. Complex **1** is unlikely to be involved, because it is favoured compared to **2** at lower temperatures and there is no extra tmen present. The observed effect might arise from the formation of a mononuclear, five-co-ordinate species such as $[FeCl_2(tmen)(thf)]$, stable on the time-scale of the experiment. However, the Fe^{II} system still appears to be ferromagnetically coupled at temperatures higher than the transition temperature and although the overall ferromagnetic effect is weak over the whole temperature range,

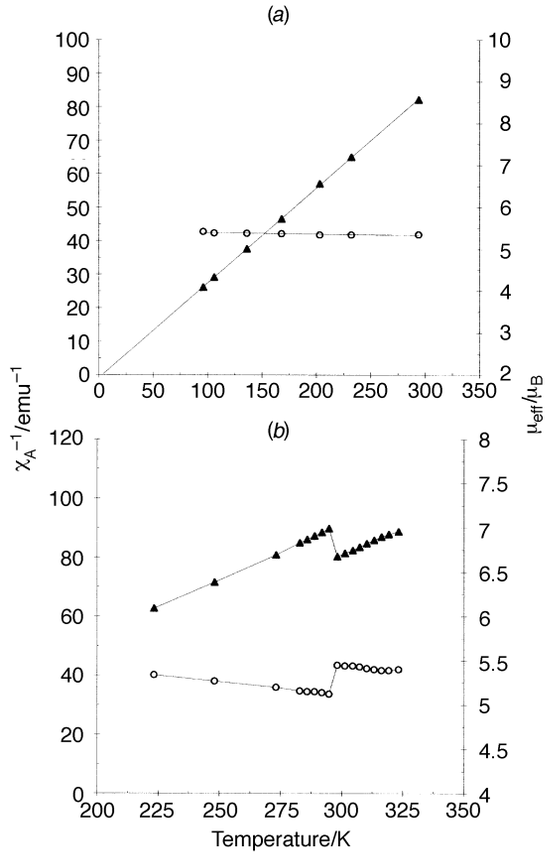

Fig. 4 Plot of the inverse of the atomic magnetic susceptibility (χ_A^{-1}, ▲) and effective magnetic moment (μ_{eff}, ○) *versus* temperature for $[\{FeCl(tmen)\}_2(\mu\text{-}Cl)_2]$ **2** (*a*) in the solid state and (*b*) in $[^2H_8]$thf solution. Diamagnetic correction: 1.342×10^{-4} emu/atom Fe^{II}

it can be rationalised only on the basis of some degree of aggregation. The conversion of **2** into a trinuclear complex such as **3** is conceivable. This happens in vanadium(II) systems, but there is no support for this here, neither from the ^1H NMR spectra of **2** or **3** at temperatures corresponding to these measurements nor from the temperature dependence of the magnetic moment/magnetic susceptibility of **3**.

In the solid state the effective magnetic moment of $[Fe_3Cl_5(tmen)_3][BPh_4]$ **3** increases from 5.4 at room temperature to 5.8 μ_B at 90 K, indicating some ferromagnetic coupling between the metal centres. The magnetic behaviour in solution was investigated in a three-step experiment (Fig. 5). The measurements were started at 293 K and repeated at 10–20 K intervals down to 173 K. The system was then warmed to 323 K, measurements being made from 278 to 323 K. Finally, the system was cooled again to 273 K. The effective magnetic moment per iron(II) ion increases with decreasing temperature, consistent with ferromagnetic coupling between iron(II) centres. The effect is reproducible though not dramatic, and is similar to the properties recently reported for some bis(μ-halogeno) dinuclear Fe^{II} complexes.[14]

No thermal hysteresis was observed in solution in the temperature range $273 < T < 323$ K. Field hysteresis, a phenomenon generally associated with the magnetic behaviour of ferromagnetic systems, could not be detected by either of the methods employed, because all measurements were carried out above the Curie temperature for the complex. In the absence of direct Fe–Fe bonds (as shown by the long M · · · M distances determined by X-ray crystallography), the ferromagnetic coupling is probably mediated by the orbitals of the bridging halides. For co-ordination compounds with bridged metal atoms such as **2** and **3**, ferromagnetism arises when the singly-occupied metal orbitals involved in the magnetic interaction are orthogonal to each other. The doubly-occupied orbitals on the

Table 5 Mössbauer parameters for complexes **1**, **2** and **3** (recorded at 77 K, referenced against iron foil at 298 K)

Compound	i.s.[a]/mm s^{-1}	q.s.[a]/mm s^{-1}	$\Gamma^{a,b}$/mm s^{-1}	% total area[a,c]
1 $[FeCl_2(tmen)_2]$	1.17(1)	3.10(1)	0.15(1)	56(2)
	1.17(1)	2.78(1)	0.15(1)	44(2)
2 $[\{FeCl(tmen)\}_2(\mu\text{-}Cl)_2]$	1.06(1)	3.12(1)	0.15(1)	39(3)
	1.06(1)	2.83(1)	0.16(1)	61(1)
3 $[Fe_3Cl_5(tmen)_3][BPh_4]$	1.14(1)	2.00(1)	0.22(1)	100

[a] Numbers in parentheses are the errors in the last significant figure. [b] Half-width at half maxima. [c] No constraints applied.

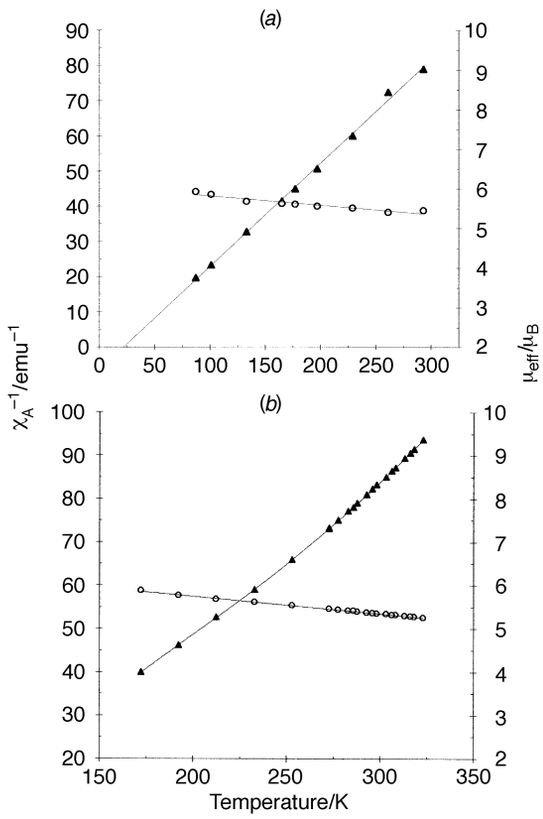

Fig. 5 Plot of the inverse of the atomic magnetic susceptibility (χ_A^{-1}, ▲) and effective magnetic moment (μ_{eff}, ○) *versus* temperature for $[FeCl_5(tmen)_3][BPh_4]$ **3** (*a*) in the solid state and (*b*) in $[^2H_8]$thf solution. Diamagnetic correction: 1.990×10^{-4} emu/atom Fe^{II}

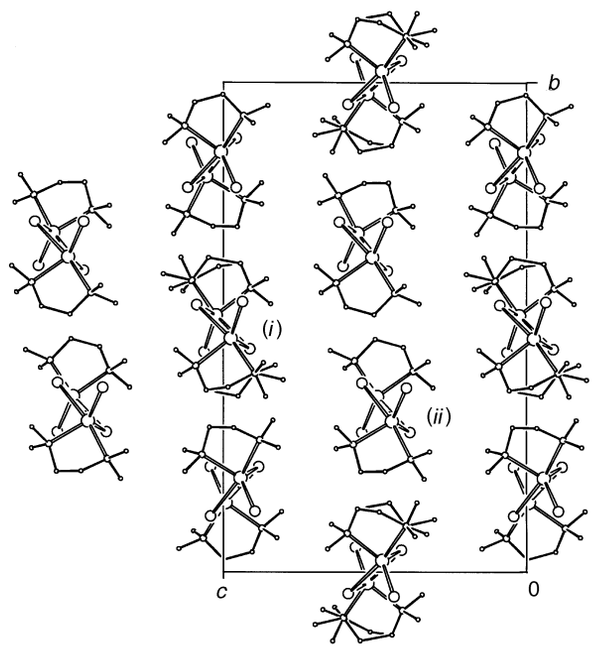

Fig. 6 Packing of the centrosymmetric (*i*) and non-centrosymmetric (*ii*) molecules of complex **2** (view down the *a* axis). The disordered methylene bridges and methyl groups of the chelating tmen molecules in the centrosymmetric dimer are depicted

bridging ligands allows the establishment of orthogonal three-electron two-centre bonds with parallel spins on the metal ions.[19]

The Mössbauer data for all three complexes, **1**, **2** and **3**, at 77 K are shown in Table 5. The spectrum for **1** can be resolved into two quadrupole doublets, which implies the presence in the solid state of two non-equivalent high-spin iron(II) species. This may be a consequence of the disorder of the di(methylene) bridges in the tmen. Crystallographically, there must be centrosymmetry averaged over all the molecules in the unit cell. However, Fig. 1 indicates four possibilities: centrosymmetric containing C(2a) and C(2a′); centrosymmetric containing C(2b) and C(2b′); non-centrosymmetric containing C(2a) and C(2b′); and non-centrosymmetric containing C(2b) and C(2a′). Therefore half the iron centres have a centrosymmetric environment and half do not. This hypothesis explains the two species present in equal amounts suggested by the Mössbauer spectrum.

The Mössbauer spectra obtained for **2** were also sharp and like that of **1** were resolved into pairs of 'nested' doublets. As with **1**, the best fit is compatible with small differences in the symmetry of the d-electron cloud around the metal nuclei in each of the two solid-state components of the crystal. The relative areas of the two doublets suggested a rough 2:1 ratio of non-equivalent iron centres, but there is no obvious reason for such non-equivalence.

Each unit cell of **2** contains four non-centrosymmetric dimers and two centrosymmetric ones, and the centrosymmetric molecule is disordered in the tmen bridges. There is a 2:1 ratio of the two types of molecule, but this cannot be the explanation of the non-equivalence of the Mössbauer parameters, because structural disorder does not imply differences in the electron density distribution at the metal.

Consideration of packing in the solid may provide a more satisfactory answer. In the packing diagram (Fig. 6) the environments of Fe(1) and Fe(1′) (in the centrosymmetric dimer) are centrosymmetric. This is because over the whole crystal there is a statistically symmetric distribution of the possible orientations of the disordered tmen ligands and each centrosymmetric dimer is symmetrically surrounded by non-centrosymmetric molecules, which are not disordered. However, there is no centre of symmetry in the Fe(2)/Fe(3) molecule (the non-centrosymmeric dimer) and the molecules surrounding this dimer are not related by any symmetry element. In addition, because of the disorder in the Fe(1)/Fe(1′) molecule, the iron centres in the non-centrosymmetric dimer can experience various environments depending upon the orientations of the tmen bridges in the nearest centrosymmetric neighbours. Therefore, the environment of Fe(2)···Fe(3) is not centrosymmetric. The 2:1 proportion holds here, because there are twice as many asymmetric surroundings as centrosymmetric ones. This could affect the symmetry of the electron density around each non-equivalent Fe nucleus, and hence the quadrupole splittings in the Mössbauer spectra.

We know of no precise analogy for the splitting of a Mössbauer signal due to asymmetric packing. However, there is at least one case in which iron atoms that might be expected to be similar do give rise to different signals. The complex [{Fe(tmen)(O_2CMe)}$_2$(μ-H_2O)(μ-O_2CMe)$_2$] is unexpectedly asymmetric in the crystal because the bridging water molecule hydrogen bonds more strongly to one iron-bound terminal carboxylate than to the other. The reason is not obvious, but the Mössbauer spectrum gives rise to two doublets, probably an electronic consequence of this asymmetry. The analogous complex with benzoate rather than of ethanoate is completely symmetrical in the crystal and gives rise to the expected single doublet in the Mössbauer spectrum.[20]

The Mössbauer spectrum of **3** was always a doublet, slightly broader than might have been expected of a single species. Attempts to fit the spectrum to a pair of 'nested' doublets were sometimes successful, although no satisfactory explanation was found for such behaviour. The lines were not sharpened by recrystallisation of the sample or by grinding the crystals with boron nitride and the broadening may be due to magnetic relaxation, which is common in high-spin Fe^{III} compounds, though not in Fe^{II}.[21]

The isomer shifts and the quadrupole splittings of **1**, **2** and **3** show the expected trends. The lower co-ordination number in the trigonal-bipyramidal **2** gives the lowest isomer shift because the s-character of the hybrid orbitals on the five-co-ordinate iron is greater. The low symmetry around iron reduces delocalisation of the d-electrons, consistent with the large quadrupole splittings. Five-co-ordinate environments are recognised to give rise to large quadrupole splittings.[22]

A combination of unique steric and electronic features makes tmen a very useful ligand for first-row transition metals such as vanadium and iron. Extensions into titanium(II),[23] chromium(II),[24] cobalt(II),[7] and manganese(II)[7] chemistry have also been made. The iron(II)–tmen complexes show that solid-state adducts of distinct nuclearities can be isolated, though they are easily interconvertible in solution. These interconversions have equivalents in V^{II} chemistry, but the thermal stability of the amine complexes seems to decrease from vanadium(II) to iron(II).

A vanadium analogue of the dinuclear complex **2** has not yet been found, neither has the tetranuclear vanadium equivalent of [$Fe_4Cl_8(thf)_6$]. Thus vanadium(II)–tmen chemistry still shows a number of big gaps. Nevertheless, the close parallels in the chemistry that we have already discovered suggest that these gaps might soon be filled, and that heteronuclear species containing both iron and vanadium should be accessible. We shall report shortly on our attempts to produce such materials.

Experimental

All operations were carried out under an inert atmosphere in a dinitrogen-filled drybox (Faircrest Engineering, Croydon) or with use of standard Schlenk techniques. Solvents were dried by standard procedures[25] and distilled under N_2 prior to use. Iron(II) chloride was synthesised from metallic iron and HCl, and sodium tetraphenylborate (Aldrich) was used as received. *N*,*N*,*N*′,*N*′-Tetramethylethylenediamine was refluxed over molten sodium for *ca.* 1 h and then distilled under N_2.

Microanalyses were carried out at the Department of Chemistry, University of Surrey, using a Leeman CE 440 CHN elemental analyser. Chlorine contents were determined by Butterworth Laboratories (Teddington, Middlesex), while iron analyses were performed by Southern Science plc, using ICP–OES.

Infrared data were recorded on a Perkin-Elmer 883 instrument, from Nujol mulls prepared under dinitrogen and spread on KBr plates. Conductivity measurements were carried out in tetrahydrofuran or dichloromethane solutions (*ca.* 10^{-3} mol dm^{-3}) using a V-shaped cell (cell constant = 1.54) connected to a Portland electronic bridge.

Mass spectra were recorded on a VG Autospec spectrometer (Fisons Instruments), equipped with a CsI gun at 25 kV (SIMS technique) or on a Kratos MS80RF machine with xenon at 8 kV (FAB technique). In both cases, 3-nitrobenzyl alcohol was used as the matrix.

Mössbauer data were recorded at 77 K on an ES-Technology MS105 spectrometer with a 25 mCi ^{57}Co source in a rhodium matrix. Spectra were referenced against iron foil at 298 K. Samples were pure solids or mixtures with boron nitride (*ca.* 50% w/w), ground to fine powders and then transferred to the aluminium sample holders in the glove box. The program used for spectra fitting and parameter calculation was ATMOSFIT 4.[26]

Magnetic susceptibility measurements were carried out in solution by variable-temperature NMR spectroscopy using the Evans method,[27] with tetramethylsilane as the marker molecule unless otherwise stated. Samples were carefully weighed under N_2, dissolved in the appropriate solvent mixture (deuteriated solvent and marker) in the glove box, and transferred to the outer tube of the coaxial NMR tube system. The solvent mixture without the paramagnetic sample was then placed in the inner tube. Spectra were recorded in the temperature range 100 to 50 °C (173–323 K) for [$^2H_8$]thf solutions.

Measurements in the solid state for the same samples were carried out at the University of Surrey, using a Newport variable-temperature Gouy balance over the range 90–295 K. The field strength was calibrated by measurements on Hg[Co(NCS)$_4$] and [Ni(en)$_3$][S_2O_3] (en = ethylenediamine); the temperature scale was checked with $CuSO_4$·$5H_2O$. Corrections were applied for the diamagnetism of the sample tubes.

Preparation of [$FeCl_2$(tmen)$_2$] 1 and [{FeCl(tmen)}$_2$(μ-Cl)$_2$] 2

To a pink suspension of anhydrous $FeCl_2$ (4.9 g, 38.5 mmol) in thf (180 cm^3) heated under reflux, an excess of tmen (18 cm^3, 13.9 g, 119.6 mmol) was added by syringe. The mixture changed to a light yellow solution. The heating under reflux was continued for 1.5 h, and the hot mixture was then filtered through Celite. A fine brown residue was separated from the light green filtrate and discarded. The solution was then concentrated under vacuum (at 30–40 °C) to *ca.* 120 cm^3 and left standing at room temperature for 20 h. Very light green thin needles of the dinuclear complex **2** were the first isolated by filtration. They were washed with thf–hexane (1:2) and dried under vacuum. Yield: 1.6 g (Found for **2**: C, 29.7; H, 6.90; N, 11.6. $C_{12}H_{32}Cl_4Fe_2N_4$ requires: C, 29.7; H, 6.65; N, 11.5%). This crystalline product is highly oxygen- and moisture-sensitive, both in solution and in solid state, changing quickly to deep brown when exposed to air.

After the isolation of **2**, the filtrate was left at room temperature for a further 5 d, giving a mixture of light green needles and colourless thick prisms. One day later, only a homogeneous batch of colourless crystals of **1** was seen. They were then filtered off without washing or extensive drying. Additional amounts of **1**, but not of **2**, were obtained upon concentration of the mother liquor and cooling at −20 °C for a few days. Yield of **1** 7.0 g (Found: C, 40.1; H, 9.30; N, 15.6. $C_{12}H_{32}Cl_3FeN_4$ requires: C, 40.1; H, 9.00; N, 15.6%). Total yield of both materials, based on the total content of Fe^{II}: 68%.

IR (Nujol mull, selected absorptions) **1**: ν(C–N) at 1011s and 1026s, ν(Fe–N) at 454m and 479m; **2**: ν(C–N) at 1009s and 1025s, ν(Fe–N) at 441m, 462m and 485m cm^{-1}. FAB mass spectra for **2** (*m*/*z*, relative intensity): 449 [{*M* − Cl}$^+$, 2], 269 (12); 207 [{FeCl(tmen)}$^+$, 13]; 117 [{Htmen}$^+$, (100)]; 72 [{$Me_2NCH_2CH_2$}$^+$, 58]; 58 [{Me_2NCH_2}$^+$, 42%].

Complex **2** was also prepared from an equimolar mixture of anhydrous $FeCl_2$ (4.1 g, 32.3 mmol) and tmen (4.9 cm^3) in refluxing thf (150 cm^3). The crystals obtained were beautiful

pale green long prisms which were washed and dried without any visible change. Yield: 6.3 g (80%). This procedure did not produce compound **1**.

Complexes **1** and **2** are soluble in thf, acetone and dichloromethane, insoluble in diethyl ether and hexane, and soluble with subsequent reaction in methanol. Neither compound is a conductor in solution in thf or CH_2Cl_2.

Preparation of $[Fe_3Cl_5(tmen)_3][BPh_4]$ 3

A colourless solution of $Na[BPh_4]$ (0.5 g, 1.5 mmol) in thf (10 cm^3) was added slowly, at room temperature, to a very light green-yellowish solution of $[FeCl_2(tmen)_2]$ **1** (1.5 g, 4.2 mmol) completely dissolved in thf (25 cm^3). The reaction was carried out for *ca.* 20 h, giving a fine light brown suspension which was then concentrated to 25 cm^3 under vacuum and filtered. The filtrate was carefully layered with 30 cm^3 of hexane and left standing at room temperature for 7 d to produce long light brown prisms; they were isolated by filtration, washed with thf–hexane (1.5:1) and dried quickly to remove the excess of solvent. These prisms, like crystals of **1**, become opaque and change to a powder when dried under vacuum. Yield: 0.9 g (64%). Purification of the product was achieved by recrystallisation from thf–hexane mixtures (Found: C, 50.1; H, 6.95; N, 8.20. $C_{42}H_{68}BCl_5Fe_3N_6$ requires: C, 49.8; H, 6.80; N, 8.30%).

Complex **3** was also synthesised in 62% yield from dinuclear **2** and $Na[BPh_4]$ under similar experimental conditions (Found: C, 49.7; H, 6.90; N, 8.40%). IR (Nujol mull): 1948w, 1878w, 1814w, 1764w; 1581ms; ν(B–aryl) at 1429s and 1424s; ν(C–N) at 1020s and 1004s; δ(C–H aromatic, out-of-plane) at 749s, 735s and 708s; ν(Fe–N) at 495m, 468m and 440m cm^{-1}. FAB mass spectrum (*m*/*z*, relative intensity): 553 (4); 269 (12); 154 (17); 136 (17); 117 [{Htmeda}$^+$, 100]; 72 [{Me_2NCH_2-CH_2}$^+$, 90]; 58 [{Me_2NCH_2}$^+$, 82%].

X-Ray diffraction analyses

***trans*-$[FeCl_2(tmen)_2]$ 1.** Crystal data: $C_{12}H_{32}Cl_2FeN_4$, M = 359.2, monoclinic, space group $P2_1/n$ (equivalent to number 14), a = 9.405(1), b = 12.333(1), c = 8.012(1) Å, β = 97.369(8)°, U = 921.7(2) Å^3, Z = 2, D_c = 1.294 g cm^{-3}, $F(000)$ = 384, μ = 11.1 cm^{-1}, λ(Mo-Kα) = 0.710 69 Å, T = 295 K.

Crystals were air sensitive, clear, colourless plates with rounded edges. One, *ca.* 0.21 × 0.45 × 0.57 mm, covered by grease and mounted in a glass capillary tube containing a small amount of tmen, was examined photographically, then transferred to an Enraf-Nonius CAD-4 diffractometer (monochromated radiation). Accurate cell parameters were determined from the settings of 25 reflections θ, in the range 10–11°, and each reflection centred in four orientations. Diffraction intensities were recorded in the ω–θ scan mode to θ_{max} = 25°.

During processing, corrections were applied for Lorentz-polarisation effects, absorption (by semiempirical ψ-scan methods) and to eliminate negative net intensities (by Bayesian statistical methods). There was no deterioration of the crystal. Of the 1621 unique reflections input into SHELX,[28] 1377 were 'observed' with $I > 2\sigma_I$. By analogy with the structure of *trans*-$[VCl_2(tmen)_2]$,[10] with which the crystals of **1** are closely isostructural, the Fe atom was placed at the origin and the remainder of the structure was located in successive difference maps.

One end of the tmen ligand bridge is disordered equally in two orientations, but the N and the methyl-C atoms have not been resolved into separate sites for the two orientations. Hydrogen atoms have been included on all the methyl-C atoms (and refined with geometrical constraints) but not on the bridging methylene groups. The non-hydrogen atoms (except for the disordered bridging-C atom) were allowed anisotropic thermal parameters. At convergence, R = 0.052 and R_g[28] = 0.074 for all 1621 reflections weighted $w = (\sigma_F^2 + 0.000\,63F^2)^{-1}$. In the final difference map, the only peak of significance, at *ca.* 0.55 e Å^{-3}, is close to the bridge of the tmen ligand.

For all the analyses, scattering factor curves for neutral atoms were taken from ref. 29. Computer programs used in this analysis have been noted above and in Table 4 of ref. 30, and were run on the MicroVAX 3600 machine in the Nitrogen Fixation Laboratory.

$[\{FeCl(tmen)\}_2(\mu\text{-}Cl)_2]$ 2. Crystal data: $C_{12}H_{32}Cl_4Fe_2N_4$, M = 485.9, monoclinic, space group $P2_1/n$ (equivalent to number 14), a = 9.9431(7), b = 23.152(2), c = 14.459(1) Å, β = 96.141(6)°, U = 3309.3(4) Å^3, Z = 6, D_c = 1.463 g cm^{-3}, $F(000)$ = 1512, μ = 18.1 cm^{-1}, λ(Mo-Kα) = 0.710 69 Å, T = 295 K.

Crystals were air sensitive, pale green prisms. Several were sealed in glass capillaries in the glove-box. One, *ca.* 0.10 × 0.10 × 0.55 mm, was examined photographically then transferred to the CAD-4 diffractometer. Accurate cell parameters were determined as described above and diffraction intensities were recorded to θ_{max} = 23°.

During processing, corrections were applied as above and for crystal deterioration (*ca.* 15% overall). Of 4585 unique reflections entered into the SHELX[28] program system, 3094 had $I > 2\sigma_I$.

The structure was determined by the automated Patterson routines in SHELXS 30 and refined by full-matrix least-squares methods in SHELXN.[28b] In one tmen ligand, there is disorder of a Me_2NCH_2 group equally in two orientations (with a common N atom site). Hydrogen atoms were included in all the tmen ligands except in the disordered group; methylene H atoms were in idealised positions, and those in methyl groups were refined with geometrical restraints. The isotropic temperature factors of all the H atoms were refined freely. All the non-hydrogen atoms, including the disordered C atoms, were allowed anisotropic thermal parameters. Refinement converged smoothly to R = 0.069 and R_g[28] = 0.076 for all 4585 reflections weighted $w = (\sigma_F^2 + 0.001\,51F^2)^{-1}$. In the final difference map, the highest peaks, at 0.8 e Å^{-3} and <0.6 e Å^{-3}, were all within the tmen ligands.

$[Fe_3Cl_5(tmen)_3][BPh_4]$ 3. Crystal data: $C_{18}H_{48}Cl_5Fe_3N_6C_{24}$-$H_{20}B$, M = 1012.7, monoclinic, space group $P2_1/n$ (equivalent to number 14): a = 19.752(2), b = 21.617(2), c = 11.977(1) Å (cell dimensions from first crystal, see below), β = 99.339(8)°, U = 5045.7(9) Å^3, Z = 4, D_c = 1.333 g cm^{-3}, $F(000)$ = 2120, μ = 11.5 cm^{-1}, λ(Mo-Kα) = 0.710 69 Å, T = 295 K.

Crystals were air sensitive, very pale yellow rectangular prisms; several were covered by grease and mounted in capillary tubes. After photographic examination, one, *ca.* 0.14 × 0.17 × 0.70 mm, was transferred to the CAD-4 diffractometer for the determination of accurate cell parameters as described above. Diffraction intensities were measured to θ_{max} = 20°, at which stage the intensities of three monitoring reflections had decreased by *ca.* 28.7%. For measurement of the data in the range 20 ⩽ θ ⩽ 25°, a second crystal, *ca.* 0.45 × 0.45 × 0.70 mm was used; this crystal deteriorated by *ca.* 8.0% during the data collection. The intensities for both crystals were corrected for Lorentz-polarisation effects and absorption (by semi-empirical ψ-scan methods) before being scaled together, merged and adjusted by Bayesian statistical methods to ensure no negative net intensities. The combined data-set of 8871 unique reflections (5011 of which had $I > 2\sigma_I$) was then entered into the SHELX program system.[28]

The structure was determined from the direct methods routines in SHELXS[31] and refined by large-block-matrix least-squares methods with a total of 690 refined parameters. All non-hydrogen atoms were allowed anisotropic thermal parameters. Hydrogen atoms of methylene and phenyl groups were included in idealised positions and were set to ride on their parent carbon atoms; those in methyl groups were refined with

geometrical constraints. The isotropic temperature factors of all the hydrogen atoms were refined independently. At completion, $R = 0.094$ and R_g [28] $= 0.077$ for all 8871 reflections weighted $w = (\sigma_F^2 + 0.0009F^2)^{-1}$. In a final difference map, the highest peaks, *ca.* 0.55 e Å^{-3}, were all close to the Fe_3Cl_5 core of the cation.

Atomic coordinates, thermal parameters, and bond lengths and angles have been deposited at the Cambridge Crystallographic Data Centre (CCDC). See Instructions for Authors, *J. Chem. Soc., Dalton Trans.*, 1997, Issue 1. Any request to the CCDC for this material should quote the full literature citation and the reference number 186/481.

Acknowledgements

We thank Mrs. J. E. Barclay and Dr. D. J. Evans for help with Mössbauer measurements and Ms. N. Walker for the microanalyses, and we are grateful for financial assistance (to J. S. de S.) from the British Council and the Brasilian Research Council (CNPq), and to the BBSRC for support.

References

1 D. L. Hughes, L. F. Larkworthy, G. J. Leigh, C. J. McGarry, J. R. Sanders, G. W. Smith and J. S. de Souza, *J. Chem. Soc., Chem. Commun.*, 1994, 2137; P. B. Hitchcock, D. L. Hughes, L. F. Larkworthy, G. J. Leigh, C. J. Marmion, J. R. Sanders, G. W. Smith and J. S. de Souza, *J. Chem. Soc., Dalton Trans.*, 1997, 1127.
2 F. A. Cotton, S. A. Duraj, L. E. Manzer and W. J. Roth, *J. Am. Chem. Soc.*, 1985, **107**, 3850.
3 R. L. Robson, R. R. Eady, T. H. Richardson, R. W. Miller, M. Hawkins and J. R. Postgate, *Nature* (*London*), 1986, **322**, 388; R. R. Eady and G. J. Leigh, *J. Chem. Soc., Dalton Trans.*, 1994, 2739.
4 D. H. Hill and A. Sen, *J. Am. Chem. Soc.*, 1988, **110**, 1650; D. H. Hill, M. A. Parvez and A. Sen, *J. Am. Chem. Soc.*, 1994, **116**, 2889.
5 D. L. Hughes, G. J. Leigh, J. R. Sanders and J. S. de Souza, unpublished work.
6 D. T. Atkinson, P. B. Hitchock and G. J. Leigh, unpublished work.
7 P. Sobota, J. Utko, S. Szafert, Z. Janas and T. Glowiak, *J. Chem. Soc., Dalton Trans.*, 1996, 3469.
8 Z. Janas, P. Sobota and T. Lis, *J. Chem. Soc., Dalton Trans.*, 1991, 2429.
9 (*a*) V. K. Bel'skii, V. M. Ishchenko, G. M. Bulychev, A. N. Protskii, G. L. Soloveichik, O. G. Ellert, Z. M. Seifulina, Yu. V. Rakitin and V. M. Novotortsev, *Inorg. Chim. Acta*, 1985, **96**, 123; (*b*) F. A. Cotton, R. L. Luck and K.-A. Son, *Inorg. Chim. Acta*, 1991, **179**, 11.
10 J. J. H. Edema, W. Stauthamer, F. van Bolhuis, S. Gambarotta, W. J. J. Smeets and A. L. Spek, *Inorg. Chem.*, 1990, **29**, 1302.
11 P. N. Hawker and M. V. Twigg, *Comprehensive Coordination Chemistry*, eds. G. Wilkinson, R. D. Gillard and J. A. McCleverty, Pergamon, Oxford, 1987, vol. 4, p. 1179.
12 Y. Hazony, R. C. Axtmann and J. W. Hurley, *Chem. Phys. Lett.*, 1968, **2**, 440.
13 John A. Dean (Editor), *Lange's Handbook of Chemistry*, McGraw-Hill, New York, 13th edn., 1985, pp. 3–121; A. M. James and M. P. Lord, *Macmillan's Chemical and Physical Data*, Macmillan, London, 1992, pp. 42–43.
14 Y. Zang, Ho G. Jang, Yu-M. Chiou, M. P. Hendrich and L. Que, *Inorg. Chim. Acta*, 1993, **213**, 41.
15 D. K. Mills, Y. M. Hsiao, P. J. Farmer, E. V. Atnip, J. H. Reibenspies and M. Y. Darensbourg, *J. Am. Chem. Soc.*, 1991, **113**, 1421.
16 A. Klose, E. Solari, C. Floriani, A. Chiesi-Villa, C. Rizzoli and N. Roe, *J. Am. Chem. Soc.*, 1994, **116**, 9123; F. A. Cotton, L. M. Daniels and C. A. Murillo, *Inorg. Chim. Acta*, 1994, **224**, 5.
17 A. R. Hermes and G. S. Girolami, *Inorg. Chem.*, 1988, **27**, 1775; M. D. Fryzuk, D. B. Leznoff, S. J. Rettig and R. C. Thompson, *Inorg. Chem.*, 1994, **33**, 5528.
18 J. S. de Souza, D. Phil. Thesis, Univesity of Sussex, 1995.
19 Ch. Elschenbroich and A. Salzer, *Organometallics*, *A Concise Introduction*, VCH, Weinheim, 1992, pp. 19, 66, 197 and 327; R. S. Drago, *Physical Methods for Chemists*, Saunders College, Philadelphia, 2nd edn., 1992, pp. 469–499.
20 K. S. Hagen and R. Lachiotte, *J. Am. Chem. Soc.*, 1992, **114**, 8741.
21 R. V. Parish, *NMR, NQR, EPR and Mössbauer Spectroscopy*, Ellis Horwood, Chichester, 1990, p. 128.
22 D. L. Hughes, M. Jimenez-Tenorio, G. J. Leigh, A. Houlton and J. Silver, *J. Chem. Soc., Dalton Trans.*, 1992, 2033.
23 J. J. H. Edema, R. Duchateau and S. Gambarotta, *Inorg. Chem.*, 1991, **30**, 154.
24 M. Dionne, S. Hao and S. Gambarotta, *Can. J. Chem.*, 1995, **73**, 1126.
25 P. D. Perrin and W. L. F. Armarego, *Purification of Laboratory Chemicals*, Pergamon, New York, 3rd edn., 1988.
26 I. Morrison, ATMDSFIT 4, University of Essex.
27 D. F. Evans, *J. Chem. Soc.*, 1959, 2003; D. F. Evans, G. V. Fazakerley and R. F. Phillips, *J. Chem. Soc. A*, 1971, 1931; D. F. Evans and T. A. James, *J. Chem. Soc., Dalton Trans.*, 1979, 723; N. V. Baker, L. D. Field and T. W. Hambley, *Inorg. Chem.*, 1988, **27**, 2872.
28 (*a*) G. M. Sheldrick, SHELX 76, Program for Crystal Structure Determination, University of Cambridge, 1976; (*b*) G. M. Sheldrick, SHELXN, an extended version of SHELX, University of Cambridge, 1977.
29 *International Tables for X-Ray Crystallograhy*, Kynoch Press, Birmingham, 1974, vol. 4, pp. 99 and 149.
30 S. N. Anderson, R. L. Richards and D. L. Hughes, *J. Chem. Soc., Dalton Trans.*, 1986, 245.
31 G. M. Sheldrick, *Acta Crystallogr., Sect. A*, 1990, **46**, 467.

Received 9*th December* 1996; *Paper* 6/08285H